JOC Article

Substituent Effects on Aryltrifluoroborate Solvolysis in Water: Implications for Suzuki−Miyaura Coupling and the Design of Stable ^{18}F-Labeled Aryltrifluoroborates for Use in PET Imaging

Richard Ting, Curtis W. Harwig, Justin Lo, Ying Li, Michael J. Adam, Thomas J. Ruth, and David M. Perrin*

Chemistry Department, University of British Columbia, 2036 Main Mall, and TRIUMF Vancouver, B.C. V6T-1Z1, Canada

dperrin@chem.ubc.ca

Received March 26, 2008

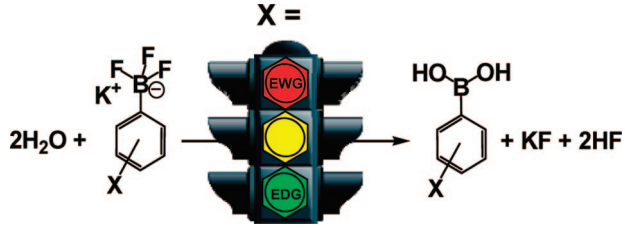

Whereas electron withdrawing substituents retard the rate of aryltrifluoroborate solvolysis, electron-donating groups enhance it. Herein is presented a Hammett analysis of the solvolytic lability of aryltrifluoroborates where $\log(k_{solv})$ values correlate to σ values with a ρ value of approximately -1. This work provides a predictable rubric for tuning the reactivity of boron for several uses including ^{18}F-labeled PET reagents and has mechanistic implications for $ArBF_3$-enhanced ligandless metal-mediated cross coupling reactions with aryltrifluoroborates.

Introduction

For nearly two decades, aryltrifluoroborates ($ArBF_3$s) have received considerable attention in Suzuki−Miyaura cross-coupling reactions.[1–7] As boronic acids/ester equivalents, $ArBF_3$s are increasingly preferred for their facile preparation from the former in aqueous KHF_2, their ready isolation via precipitation from water- and ether-miscible solvents (e.g., alcohols, acetonitrile, acetone), and their resistance to either oxidation or boroxine formation. Many of these desirable characteristics have been attributed to the alleged stability of the $ArBF_3$, which, in turn, is ascribed to the exceptional strength of the B−F bond (∼140 kcal/mol). Nevertheless, under sufficiently dilute conditions, an isolated $ArBF_3$ must suffer thermodynamically favorable and kinetically irreversible solvolysis that restores the arylboronic acid and free fluoride, for which the free energy of solvation in water is calculated to be at least on par with that of B−F bond formation.[8]

In addition to the extensive reports on the use of $ArBF_3$s in synthetic chemistry, at least one report has suggested that $ArBF_3$s may act as protease inhibitors,[9] whereas another suggested that arylboronic acids could be useful captors of aqueous [^{18}F]-fluoride that would conveniently provide ^{18}F-labeled PET-imaging agents by virtue of a pendant ^{18}F-containing $ArBF_3$.[10] Because *in vivo* use of $ArBF_3$s as pharmaceuticals and radiopharmaceuticals demands dilution to micromolar levels or lower, resistance to solvolytic defluoridation would be of paramount importance. Conversely, for Pd-catalyzed cross-couplings, which are run in aqueous cosolvents such as methanol, dimethylformamide, tetrahydrofuran, or acetonitrile at moderate-to-high concentrations of $ArBF_3$ (10−100 mM), it has been postulated that defluoridation necessarily precedes metalation.[1,11]

(1) Molander, G. A. Biolatto B. *J. Org. Chem.* **2003**, *68*, 4302–4314.
(2) Wright, S. W.; Hageman, D. L.; McClure, L. D. *J. Org. Chem.* **1994**, *59*, 6095–6097.
(3) Vedejs, E.; Chapman, R. W.; Fields, S. C.; Lin, S.; Schrimpf, M. R. *J. Org. Chem.* **1995**, *60*, 3020–3027.
(4) Molander, G. A.; Bernardi, C. R. *J. Org. Chem.* **2002**, *67*, 8424–8429.
(5) Batey, R. A.; Quach, T. D. *Tetrahedron Lett.* **2001**, *42*, 9099–9103.
(6) Darses, S.; Genet, J.-P. *Chem. Rev.* **2008**, *108*, 288–325.
(7) Stefani, H. A.; Cella, R.; Vieira, A. S. *Tetrahedron* **2007**, *63*, 3623–3658.
(8) Zhan, C.-G.; Dixon, D. A. *J. Phys. Chem. A* **2004**, *108*, 2020–2029.
(9) Smoum, R.; Rubinstein, A.; Srebnik, M. *Org. Biomol. Chem.* **2005**, *3*, 941–944.
(10) Ting, R.; et al, *J. Am. Chem. Soc.* **2005**, *127*, 13094–13095.
(11) Barder, T. E.; Buchwald, S. L. *Org. Lett.* **2004**, *6*, 2649–2652.

10.1021/jo800681d CCC: $40.75
Published on Web 05/20/2008

SCHEME 1. Minimal Kinetic Scheme for $ArBF_3$ Solvolysis Where All Steps Are Taken To Be Reversible[a]

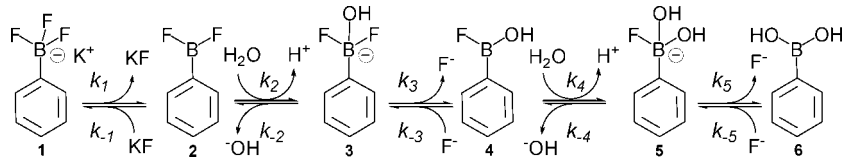

[a] Not shown are all ionized states for **3**−**5**, or a tautomer of **4**, all of which may also react such that this scheme is complicated by branched pathways. The pH-dependent hydration of the arylboronic acid to the arylborate is also not shown.

Thus, characterization of substituent effects that govern the kinetics of solvolytic loss of fluoride ion would have broad mechanistic significance for the use of $ArBF_3$s in numerous applications. Whereas Anbar and Guttmann found the notoriously inert tetrafluoroborate to solvolyze very slowly in water ($t_{1/2} \approx 168$ h, 100 °C) in a study that highlighted the strength of the B−F bond,[12] to date, the aqueous stabilities of a few $ArBF_3$s have been but briefly described with only brief mention made of their allegedly high aqueous stability.[13–15] There exists neither a quantitative measure of the solvolytic lability of an $ArBF_3$ nor any knowledge as to how electronic structure would influence it. Herein, we use both NMR spectroscopy and $^{18}F/^{19}F$-fluoride isotopic exchange autoradiography in this first study that quantitatively measures the rate constant for solvolysis, k_{obs}, which can be fit to a simple first-order equation and which depends quite reliably on the electronic nature of substituent effects at the *meta* and *para* positions.

Results

In studying the solvolysis of $ArBF_3$s, we initially considered both the forward and reverse reactions shown schematically in Scheme 1. *A priori*, at high concentrations of $ArBF_3$, one must entertain a difficult set of presteady-state differential equations to account for product inhibition due to HF evolution and the feedback effects of solvent pH depression in the absence of buffer. To simplify this scheme, we chose to study solvolysis under conditions that would (i) be relevant to those commonly used by researchers working with $ArBF_3$s (e.g., aqueous buffered conditions) and (ii) simplify the kinetic analysis.

We chose not to treat the kinetics of $ArBF_3$ formation because $ArBF_3$s are generally formed under one set of conditions (usually molar concentrations of $ArB(OR)_2$ and KHF_2, low pH, R = H, alkyl) and then used for coupling or *in vivo* targeting under other more dilute conditions: for the former at moderate dilution (1−100 mM) in mixed aqueous media (pH 8−10 adjusted with K_2CO_3), or for the latter at very high intravenous dilution (blood, pH 7.4). Thus for both uses, solvolytic loss of fluoride, starting with the *first* fluorine atom, would arguably be considered the most important step because this step is on the one hand thought to be *essential* for transmetalation in Pd-catalyzed cross coupling[16–18] and on the other thought to be *undesirable* if an $ArBF_3$ is to be contemplated for *in vivo* imaging.

Thus we chose conditions of reasonable dilution (∼5 mM $ArBF_3$) that would favor the forward hydrolysis reaction and disfavor the back reaction of fluoride recapture. For similar reasons, we used phosphate buffer at a pH close to neutrality to minimize the effects of HF evolution, which would also enhance a back reaction and only diminish the observed rate of solvolysis. Our interests in the biological applications of $ArBF_3$s led us to investigate solvolysis in aqueous 192 mM phosphate buffer pH 6.9−7.0. In this initial study, we did not treat the effects of less polar cosolvents such as methanol, THF, and DMF, which are often used in metal coupling reactions. Under these chosen conditions, the kinetics simplify to the reaction shown in Scheme 2 (see the Supporting Information for a more elaborate pathway).[19]

SCHEME 2. Irreversible Kinetic Scheme for $ArBF_3$ Solvolysis under Buffered Conditions at Relatively High Dilution[a]

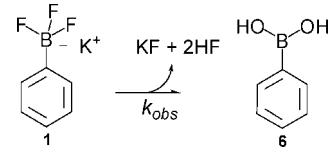

[a] Not shown are the fleeting intermediates **2**−**5** from Scheme 1, nor additional ionized states for **3**−**5** which may react differently according to the ionization state.

In Scheme 2, fluoride release is governed by a single rate-limiting step, without detection of any intermediates shown in Scheme 1. If any of intermediates **2**−**5** were to accumulate due to at least one more slow step then (i) the rate of fluoride release could be stepwise, (i.e., biphasic or triphasic), sigmoidal, or even more complicated, and (ii) ^{19}F NMR spectroscopy would identify the steady-state accumulation of another boron-bound fluoridated intermediate. Nonetheless, no intermediate is observed and both the time-dependent appearance of free fluoride and the disappearance of the $ArBF_3$ is pseudofirst order where k_{obs} approximates k_1, which must be much smaller than all other rate constants (i.e., $k_1 \ll k_2 \approx k_3 \approx k_4 \approx k_5$) that govern intermediate solvolysis. The use of low concentrations of $ArBF_3$ (qualitatively reflective of *in vivo* conditions) not only simplified the kinetics but ensured that the k_{obs} we report represents the *maxmium* observable value since it is not diminished by the presence of intermediate products that might accumulate at higher initial concentrations of $ArBF_3$ (e.g., ∼100 mM used during Pd-coupling).

We measured solvolysis by 300 MHz ^{19}F NMR spectroscopy that is sensitive enough to detect ^{19}F-chemical shifts that would correspond to the starting $ArBF_3$, any possible mono- and difluorinated intermediates, and free fluoride. ^{11}B NMR spectroscopy proved less reliable because considerably more sample was required and we wished to work at low millimolar concentrations. In this study, all $ArBF_3$s were prepared from

(12) Anbar, M.; Guttmann, S. *J. Phys. Chem.* **1960**, *64*, 1896–1899.
(13) Yuen, A. K. L.; Hutton, C. A. *Tetrahedron Lett.* **2005**, *46*, 7899–7903.
(14) Moreno-Manas, M.; Perez, M.; Pleixats, R. *J. Org. Chem.* **1996**, *61*, 2346–2351.
(15) Smoum, R.; Rubinstein, A.; Srebnik, M. *Org. Biomol. Chem.* **2005**, *3*, 941–944.
(16) Molander, G. A.; Biolatto, B. *J. Org. Chem.* **2003**, *68*, 4302–4314.
(17) Molander, G.; Biolatto, B. *Org. Lett.* **2002**, *4*, 1867–1870.
(18) Barder, T. E.; Buchwald, S. L. *Org. Lett.* **2004**, *6*, 2649–2652.

(19) Although **2** could lose a fluoride directly via a borfluoronium ion, which would hydrate to **4**; likewise **4** could lose a fluoride directly via a boroxyl, which would hydrate to **6** (see the Supporting Information).

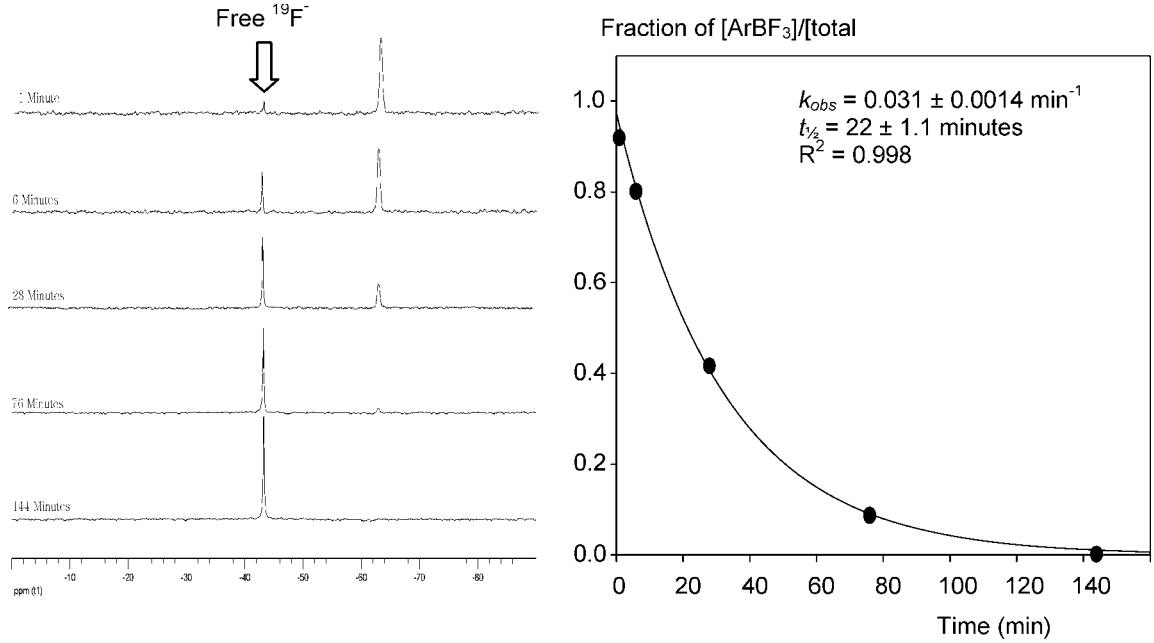

FIGURE 1. Left: ^{19}F NMR spectra of *p*-sulfonamidophenyltrifluoroborate solvolysis at 1, 6, 28, 76, and 144 min. Right: Exponential fit of the NMR spectral data.

arylboronic acids, purified, and characterized by ^{1}H and ^{19}F NMR spectroscopy in CD_3OD or DMSO-d_6 (see the Supporting Information). At 2−10 mM $ArBF_3$, the buffer (192 mM phosphate pH 6.9−7.0) neutralized the 2 equiv of evolved HF. An example of such kinetics is shown in Figure 1 where the integration values for *p*-NH_2SO_2-φ-BF_3 (ca. −65 ppm) and free fluoride (ca. −40 ppm) were fit to the equation $([ArBF_3]/([ArBF_3] + [F]))_t = ([ArBF_3]/([ArBF_3] + [F]))_0 e^{-kt}$.

In no case did we observe any steady-state intermediate corresponding to **2**−**5** by ^{19}F NMR spectroscopy. That **2** went undetected was expected since it is a difluoroborane, a species that readily smolders in moist air.[20–26] Thus, **2** must hydrate instantaneously to give intermediate **3** at pH 7, which was also not observed as it would eliminate HF to give an arylfluoroboronic acid (i.e., **4**), which should be equally reactive as **2** due to the fact that **4** shares many electronic similarities with benzoylfluoride, its carbon analogue. Because it is difficult to characterize that which cannot be readily observed, these intermediates (and possibly others not drawn) are fleeting, at least on the ^{19}F NMR time scale, and consistent with a kinetic model where the total solvolysis of a dilute $ArBF_3$ is governed by dissociation of the first fluoride in a single rate-limiting step that is best approximated by pseudofirst order kinetics.[27]

Since some free fluoride (≤1 equiv) was occasionally present in some of the $ArBF_3$ preparations from the outset,[28] we deliberately added 100 mM fluoride to the solvolysis reaction with *p*-sulfonamidophenyltrifluoroborate to investigate the effect that excess fluoride, which represents product, would have on the reaction. The value for k_{obs} in the presence of fluoride was approximately 60% of that in the absence of excess fluoride (Figure 2).

This small rate depression may be explained either by a specific reaction of fluoride with intermediate **2** forcing it back to starting material or by a medium effect related to an increase in ionic strength, or both. Although medium effects were not investigated further, it is clear that the addition of excess fluoride at 100 mM did not reveal any intermediates (**2**−**5**) and had little overall effect on the kinetic or thermodynamic stability of the $ArBF_3$.

To independently address the rate of fluoride loss, we prepared the *p*-sulfonamidophenyltrifluoroborate in the presence of trace [^{18}F]-fluoride. After an hour of synthesis, the crude reaction was diluted 200-fold in 100 mM [^{19}F]-KF and 192 mM phosphate buffer pH 6.9−7.0 and allowed to solvolyze for various periods of time. A volume of 1 μL from each exchange reaction was then spotted on a TLC plate. The large excess of [^{19}F]-KF present prevented any recapture of [^{18}F]-fluoride by the hydrolyzed arylboronic acid as the TLC plate dried.

In the absence of any antecedent report on chromatographic resolution of an $ArBF_3$ on silica, we were delighted to find that 5:95 NH_4OH:EtOH cleanly separated all [^{18}F]-$ArBF_3$ (R_f of ∼0.9) from free [^{18}F]-fluoride on standard silica with the exception of the *p*-trimethylammoniophenyltrifluoroborate.[29] This clean separation permitted autoradiography and phosphorimaged densitometry analysis of the time-dependent decrease in [^{18}F]-$ArBF_3$ and increase in the relative amount of free [^{18}F]-

(20) McCusker, P. A.; Kilzer, S. M. L. *J. Am. Chem. Soc.* **1960**, *82*, 372–375.
(21) McCusker, P. A.; Glunz, L. J. *J. Am. Chem. Soc.* **1955**, *77*, 4253–4255.
(22) McCusker, P. A.; Makowski, H. S. *J. Am. Chem. Soc.* **1957**, *79*, 5185–5188.
(23) Kinder, D. H.; Katzenellenbogen, J. A. *J. Med. Chem.* **1985**, *28*, 1917–1925.
(24) Vedejs, E.; Chapman, R. W.; Fields, S. C.; Lin, S.; Schrimpf, M. R. *J. Org. Chem.* **1995**, *60*, 3020–3027.
(25) Frohn, H.-J.; et al, *J. Organomet. Chem.* **2000**, *598*, 127–135.
(26) Chase, P. A.; Henderson, L. D.; Piers, W. E.; Parvez, M.; Clegg, W.; Elsegood, M. R. J. *Organometallics* **2006**, *25*, 349–357.
(27) An independent run was conducted in phosphate buffer at pH 7.5 with no appreciable difference in k_{obs}: $k_{obs} = (2.88 \pm 0.08) \times 10^{-2}$ min^{-1}.

(28) Most of the $ArBF_3$s were prepared by simple precipitation from methanol, acetone, or acetonitrile, and consequently some residual fluoride was also present.
(29) A ∼5 mg synthesis of trace [^{18}F]-labeled *p*-carboxyphenyltrifluoroborate was prepared by running the crude fluoridation reaction through a 0.6 g, 230−400 mesh, silica plug and collecting 100 μL fractions. Fractions 4−10 were verified by autoradiography following TLC analysis in the same solvent and were pooled, decayed and analyzed by ^{19}F NMR spectroscopy to demonstrate that these fractions were indeed the $ArBF_3$ (data not shown).

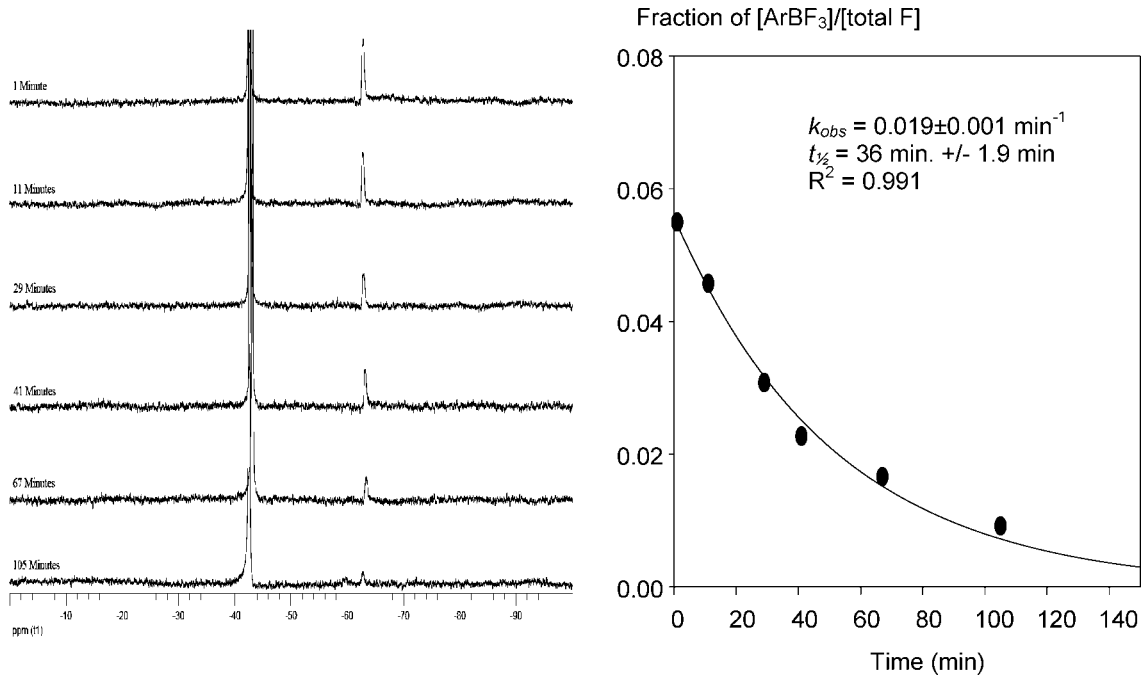

FIGURE 2. Left:[19]F NMR spectra of *p*-sulfonamidophenyltrifluoroborate solvolysis in the presence of 100 mM KF at 1, 11, 29, 41, 67, and 105 min. Right: Exponential fit of the NMR spectral data.

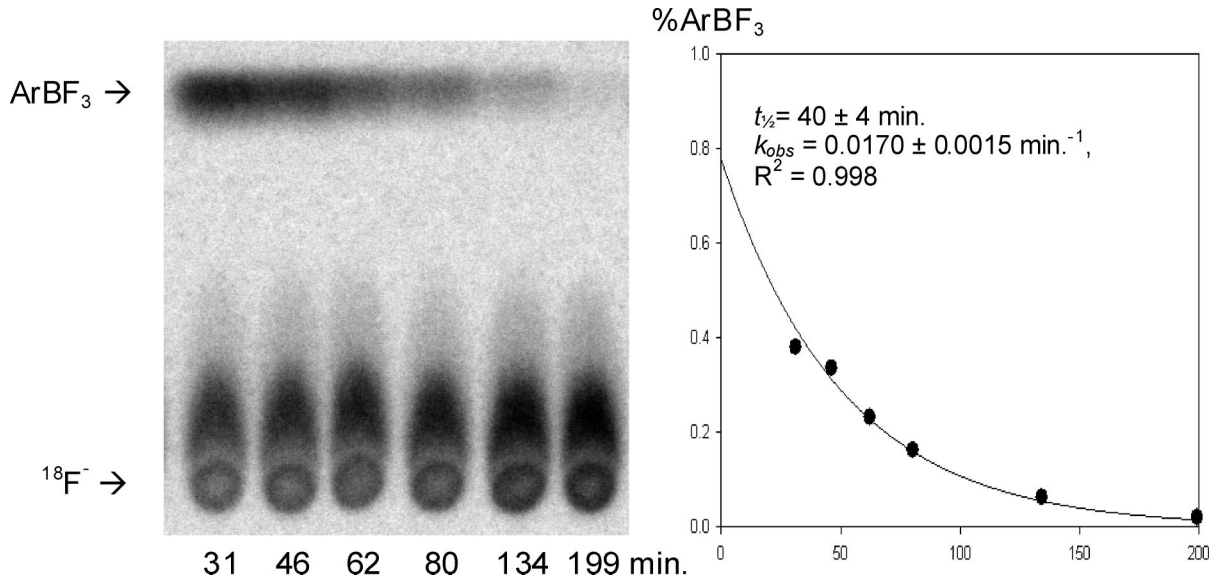

FIGURE 3. Left: Autoradiogram of time-dependent loss of *p*-sulfonamidophenyl-[^{18}F]trifluoroborate at 31, 46, 80, 134, and 199 min. Right: First-order exponential fit of the autoradiographic densitometry data.

fluoride as featured in Figure 3. The autoradiographic density corresponding to the $ArBF_3$ spot was divided by the sum of the total density, comprising $ArBF_3$ and free fluoride, to calculate the fraction of density corresponding to the $ArBF_3$. This treatment normalizes against variance in the total ^{18}F-decay intensities in each sample that is spotted on the TLC plate. The ratio of [^{18}F]-$ArBF_3$ to the total [^{18}F]-fluoride signal for each sample is plotted against time in the following equation: $[P]_t = [P]_0(e^{-k_{obs}t})$, where $[P]_t$ and $[P]_0$ are the ratios of boron-bound [^{18}F]-fluoride/total [^{18}F]-fluoride at time t and 0 min, respectively, and k_{obs} is the observed first-order rate constant for loss of [^{18}F]-fluoride from the [^{18}F]-$ArBF_3$.

The value of k_{obs} determined from the ^{18}F-autoradiographic analysis nicely corroborated that determined by ^{19}F NMR spectroscopy in the presence of 100 mM fluoride. Thus, both assays identified similar rate constants for the overall solvolysis reaction that proceeds without observable intermediates.

In contemplating the mechanism of hydrolysis, we hypothesized that loss of fluoride with concomitant vacation of the empty p-orbital on boron to give an ephemeral difluoroborane (**2**) would be stabilized by electron-donating groups at the *para* position. Hence, we hypothesized that such an effect bore analogy to other systems that had been previously investigated. For instance, the benzotrifluoride carbon analogues, namely *p*-triffluoromethylaniline [CAS registry no. 455-14-1] and *p*-trifluoromethylphenol [CAS registry no. 402-45-9], are commercially available and relatively shelf stable.[30] Although their sensitivity to solvolytic defluorination, particularly under basic

(30) Stahly, G. P.; Bell, D. R. *J. Org. Chem.* **1989**, *54*, 2873–2877.

conditions, was noted as early as 1947,[31] scant mention of their base sensitivity is found.[32–36] Only very recently have molecular dynamics calculations corroborated the difluoroquinonemethide resonance form hypothesized early on by Roberts[37] for these systems and for which kinetic analysis showed that defluorination of *p*-trifluoromethylphenol is first order.[38] These results mirror our findings. Nevertheless, to the best of our knowledge, no study has systematically studied the effects of *para* and *meta* substitution on the rate of benzotrifluoride hydrolysis, perhaps in part because the trifluoromethyl group is particularly resistant to solvolysis and only EDG-modified compositions can be readily studied. On the other hand, more comprehensive investigations had been undertaken for the solvolysis of benzyltosylates[39] and cumylchlorides,[40,41] which is enhanced via resonance effects of electron-donating groups (EDGs) at the *para* position, and retarded via respective inductive and resonance effects of electron-withdrawing groups (EWGs) at *meta* and *para* positions (Scheme 3).

SCHEME 3. (Left) *p*-EDG Resonance Stabilization of the Difluoroborane 2 and (Right) Analogous Para-Substituted Resonance Stabilization of Either a Difluorobenzyl Cation or a Cumyl Cation via a Quinonemethide-like Form

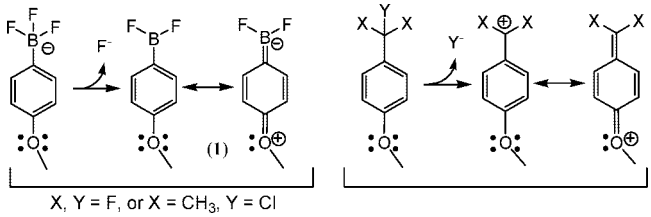

We asked if the same effect would be seen for $ArBF_3$s. To test this hypothesis, we prepared over 15 mono/disubstituted $ArBF_3$s (e.g., −Cl, −F, $-CF_3$, $-NO_2$, −CN, etc., see the Supporting Information) and followed their solvolysis to completion. In all cases, no $ArBF_3$ remained at equilibrium and no intermediates were observed. For most samples, the rate constants from both ^{19}F NMR and ^{18}F-positron TLC autoradiography were tabulated in Table 1 (p 47 of the Supporting Information), and the log(k_{obs}) was plotted vs σ_p, σ_m, or $\sigma_p + \sigma_m$ for disubstituted compositions as shown in Figure 4.[42]

Further consideration of these data, and in particular the somewhat lower correlation coefficients (*R* values), suggested several other treatments. The first retreatment of the data was to recognize that the rate constant for solvolysis in 100 mM fluoride was depressed by about a factor of 0.6 compared to that observed in buffer alone, at least for the *p*-sulfonamidophenyltrifluoroborate. This led us to normalize the rate constants

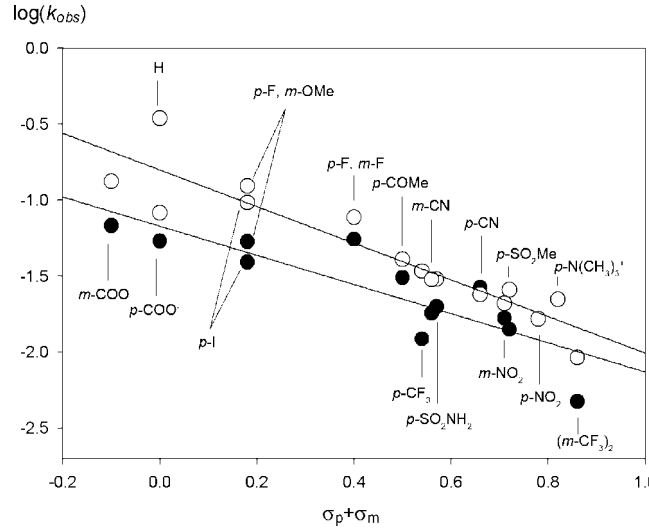

FIGURE 4. Hammett plot log(k_{obs}) = $\sigma_{(m+p)}\rho$ + log(k_0) for data in Table 1 (Supporting Information). Linear regression analysis of the log(k_{obs}) values from the $^{18/19}F$ exchange TLC (●, black line) gave a ρ value of -0.96 ± 0.15 ($R = 0.85$); of the log(k_{obs}) values from ^{19}F NMR spectroscopy kinetics (○, blue line) gave a ρ value of -1.21 ± 0.13 ($R = 0.93$); plotting σ^+ values,[43] for which there are fewer given values, gave higher *R* values (0.91−0.94) and lower ρ values: $\rho = -0.89$ (●, black line) and $\rho = -1.10$ (○ blue line) (see the Supporting Information).

obtained from the TLC-autoradiography to those obtained by ^{19}F NMR spectroscopy by adding the value of −0.21 (i.e., log(0.6)) to each and then replotting σ^+ vs both sets of values for log(k_{obs}), which gave a value of $\rho = -1.0 \pm 0.08$, and a very respectable value of *R* of 0.92 (data not shown). Finally, because it seemed reasonable that EDGs at the *para* position would distribute electron density into an empty p-orbital in the transition state, we treated the data in terms of a Yukawa−Tsuno plot (log(k_{obs}) = ($\rho\sigma^+ - R'\Delta\sigma$), where $R' = \rho r$ and $\Delta\sigma = \sigma^+ - \sigma$). Subjecting the ^{19}F NMR spectral data to a Yukawa−Tsuno analysis afforded the following values: $\rho = -1.14 \pm 0.13$, $R' = 0.36 \pm 0.53$, and a correlation coefficient of 0.94. Likewise, the ^{19}F TLC data afforded the following values: $\rho = -0.81 \pm 0.16$, $R' = -0.43 \pm 0.56$, and a correlation coefficient of 0.91. Subjecting both sets of data, where the TLC data were normalized to those of the NMR spectral data by a factor of 0.6, to a Yukawa−Tsuno analysis gave the following values: $\rho = -1.01 \pm 0.1$, $R' = 0.03 \pm 0.38$, and a correlation coefficient of 0.92. The implications of these findings are briefly discussed in the next section.

The effect of *ortho*-substitution with EDGs was briefly investigated and remains complicated: resonance activates while sterics and induction deactivate. Whereas the *p*-MeO-φ-BF_3 solvolyzed so rapidly that reliable values for k_{solv} could not be obtained, the *o*-MeO-φ-BF_3 and the 2,4-diMeO-φ-BF_3 exhibited $t_{1/2}$ values of ∼20 and ∼4 min, respectively. Likewise, the 2,4-difluoro-φ-BF_3 behaved similarly to the 2-fluoro-φ-BF_3 (see Table 1, Supporting Information). Although these *ortho* effects were not included in the σ-plot, qualitatively, *ortho*-substitution with certain groups (e.g., −F, $-CF_3$, −CN) should impart significantly increased aqueous stability to the $ArBF_3$.

Discussion of Results

This work represents the first full investigation of the effects of *meta*- and *para*- substitution on the solvolytic lability of an

(31) Jones, R. G. *J. Am. Chem. Soc.* **1947**, *69*, 2346–2350.
(32) Roberts, J. D.; Webb, R. L.; McElhill, E. A. *J. Am. Chem. Soc.* **1950**, *72*, 408–411.
(33) Bornstein, J.; Leone, S. A.; Sullivan, W. F.; Bennett, O. F. *J. Am. Chem. Soc.* **1957**, *79*, 1745–1748.
(34) Filler, R.; Novar, H. *J. Org. Chem.* **1961**, *26*, 2707–2710.
(35) Sakai, T. T.; Santi, D. V. *J. Med. Chem.* **1973**, *16*, 1079–1084.
(36) Tickner, D.; Kasthurikrishnan, N. *Org. Process Res. Dev.* **2001**, *5*, 270–271.
(37) Roberts, J. D.; Webb, R. L.; McElhill, E. A. *J. Am. Chem. Soc.* **1950**, *72*, 408–411.
(38) Reinscheid, U. M.; Vervoort, J.; Zuilhof, H. *Chemosphere* **2006**, *65*, 318–323.
(39) Kochi, J. K.; Hammond, G. S. *J. Am. Chem. Soc.* **1953**, *75*, 3445–3451.
(40) Okamoto, Y.; Inukai, T.; Brown, H. C. *J. Am. Chem. Soc.* **1958**, *80*, 4969–4972.
(41) Brown, H. C.; Okamoto, Y. *J. Am. Chem. Soc.* **1958**, *80*, 4979–4987.
(42) Hansch, C.; et al, *J. Med. Chem.* **1973**, *16*, 1207–1216.
(43) Hansch, C. *J. Med. Chem.* **1970**, *13*, 964–966.

$ArBF_3$, paralleling prior studies on the solvolysis of EDG-substituted benzotrifluorides and EDG/EWG-substituted cumylchlorides. Whereas the ρ value for cumylchloride solvolysis is ca. -4,[8] and that for benzyltosylate solvolysis in ethanol:water is ca. -2.0, the ρ value for a $ArBF_3$ in 100% buffered water is ca. -1. Indeed, a lower ρ value might be expected in part because of the greater stability of the sp^2-hybridized borane (**1**), which draws less electron density from the aromatic ring compared to a highly deficient sp^2-hybridized carbocation.

As the B−F bond is one of the strongest single bonds between any two atoms on the periodic table, the lability of EDG-substituted $ArBF_3$s was unforeseen, even if not entirely surprising once fully investigated. In light of these data, and by analogy to EDG-substituted benzotrifluorides, benzyltosylates, and cumylchlorides, resonance overlap from the EDG into the aromatic ring weakens the B−F bond strength significantly, and henceforth predictably. The effects of *para*- and *meta*-substitution with EWGs on k_{solv} also trend in accordance with σ values.

Thus, Hammett plots of $\log(k_{obs})$ vs both σ and σ^+ values were undertaken for each set of data, and in addition, a plot of σ^+ vs a combined set of $\log(k_{obs})$ values comprising both the rate constants generated by ^{19}F NMR spectroscopy and those generated by ^{18}F TLC-autoradiography that were normalized to the former. In all of these analyses, ρ values were approximately -1.0 and correlation coefficients were about 0.9. We also performed a Yukawa−Tsuno analysis[44–46] to address the hypothesis that partial electron density delocalized through the aromatic ring into the empty p-orbital on boron to enhance the rate of fluoride dissociation. This linear regression analysis improved correlation coefficients slightly but provided little insight into a meaningful quantitative relation between σ/σ^+ values and the extent of transition state electron density delocalization into the boron p-orbital as the errors attributed to R' were as large as R' itself.

In the treatments we attempted, the correlation coefficients describing goodness of fit are roughly 0.9, which indicates a respectable fit, although not as good as others. Nevertheless, we examined 13−16 different samples which represent a somewhat larger number of substituents than is often investigated in other Hammett analyses. Values that deviate from the correlated line can be attributed to several factors: (1) errors associated with measuring k_{obs}, (2) mechanistic differences (e.g., S_N1 vs S_N2) that might be attributed to a deviant analogue in question, or (3) the possibility that the σ/σ^+ values which had been assigned for the ionization of a series of benzoic acids are simply less applicable to this case.

In terms of error related to the calculation of k_{obs}, greater error is likely to be associated with the k_{obs} values obtained from compounds that solvolyze rapidly on the NMR/TLC time scale—in fact the *p*-methoxyphenyltrifluoroborate and *p*-methylthiophenyltrifluoroborate solvolyzed so rapidly that their rate constants could not be reliably measured (data not shown). Nevertheless, plotting $\log(k_{obs})$ vs σ/σ^+ values for only the slow-to-solvolyze compounds did not greatly improve the correlation coefficients. Interestingly, the *p*-trifluoromethylphenyltrifluoroborate and the *m*-di(trifluoromethyl)phenyltrifluoroborate, which are slow to solvolyze, deviate quite distinctly from the correlated line. No plausible explanation appears forthcoming for this observation other than the Hammett σ/σ^+ values may not be fully appropriate in this analysis. Furthermore, as previously noted, a Yukawa−Tsuno treatment did not shed light on the extent to which electron donation resonates across the aromatic ring to fill the vacant p-orbital on boron. Thus, we are left to conclude that the correlation is somewhat less pronounced than that for other reaction classes that are more neatly correlated because of a greater connection to substituted benzoic acids. Nevertheless, the correlations are sufficiently high to be of predictive value regarding the aqueous stability of *para*- and *meta*-substituted $ArBF_3$s stability of $ArBF_3$s, which have heretofore been undefined.

Conclusions Regarding Metal Couplings and PET Agent Design. The proclivity by which an $ArBF_3$ loses a fluoride ion has implications for several applications including metal cross couplings where solvolysis is thought to precede metalation,[47,48] and the design of humorally stable PET-imaging agents. With regards to metal coupling, this work demonstrates that for cases involving *p*-EDG-modified $ArBF_3$s in buffered water, e.g., (*p*-CH_3O-phenyltrifluoroborate), the $ArBF_3$ is likely to be entirely defluoridated within minutes of solvation.[49] On the other hand, the stability of certain EWG-modified $ArBF_3$s will be formidable, and these stabilities are likely to be further enhanced by the presence of less polar cosolvents that are commonly used in mixed aqueous conditions.

Indeed, such is not altogether inconsistent with observations that EWG-modified $ArBF_3$s are generally poorer substrates for Pd-catalyzed cross couplings. For instance, Kabalka et al. have found that whereas a Baylis−Hillman-type coupling of a phenyltrifluoroborate yields 86% in 3 h., the same coupling using the 2,6-difluorophenyltrifluoroborate yields 68% in 48 h.[50] Similar differences have been seen by Molander et al. for another Suzuki−Miyaura coupling with EWG-substituted $ArBF_3$s.[51] This observed rate depression is consistent with both our findings and the suggestion that defluoridation precedes transmetalation. Nevertheless, if in certain cases rate constants for coupling exceed the value of k_{obs} identified here for solvolysis, one may have to reconsider this assumption.

The Hammett relationship between k_{obs} for solvolysis and substituent effects also bodes well for the rational design of an assortment of PET-suitable $ArBF_3$s, which builds on our earlier work toward that goal. In 2005, we suggested the use of $ArBF_3$s for use in PET imaging based on earlier reports that had emphasized the aqueous stability of $ArBF_3$s in water, and from inference of Anbar and Guttmann's early work on the extreme sluggishness of BF_4^- solvolysis. Our communication in the Journal of the American Chemical Society employed an ^{18}F-labeled biotinylated-$ArBF_3$ to suggest a radically different approach to ^{18}F-labeling that exploited the fluorophilicity of arylboronic acids/esters as captors of aqueous [^{18}F]-fluoride that would circumvent the standard practice of generating arylfluorides in multistep labeling procedures.[52]

Thus, our initial investigation used a convenient bioconjugate, biotinamidophenylboronyl pinacolate,[53] which we designed to address the capture of radioactive [^{18}F]-fluoride whereby the

(44) $\log(k_{obs}) = \rho\sigma^+ - R'\Delta\sigma$, where $R' = \rho\sigma r$ and $\Delta\sigma = \sigma^+ - \sigma$.
(45) Tsuno, Y.; Fujio, M. *Chem. Soc. Rev.* **1996**, *25*, 129–139.
(46) Yukawa, Y.; Tsuno, Y. *Bull. Chem. Soc. Jpn.* **1959**, *32*, 965–970.
(47) Molander, G.; Biolatto, B. *Org. Lett.* **2002**, *4*, 1867–1870.
(48) Barder, T. E.; Buchwald, S. L. *Org. Lett.* **2004**, *6*, 2649–2652.
(49) Sakurai, H.; Tsunoyama, H.; Tsukuda, T. *J. Organomet. Chem.* **2007**, *692*, 368–374.
(50) Kabalka, G. W.; Venkataiah, B.; Dong, G. *Org. Lett.* **2003**, *5*, 3803–3805.
(51) Molander, G. A.; Fumagalli, T. *J. Org. Chem.* **2006**, *71*, 5743–5747.
(52) Lasne, M. C.; Perrio, C.; Rouden, J.; Barre, L.; Roeda, D.; Dolle, F.; Crouzel, C. *Top. Curr. Chem.* **2002**, *222*, 201–258.
(53) Reference 10.

biotin appendage enabled affinity chromatography on avidin-magnetic particles such that radioactive free [^{18}F]-fluoride could be removed by repeated washings. In that context we observed specific labeling of the avidin- magnetic particles in a manner that was resistant to washing and did not exchange its [^{18}F]-fluoride in the presence of added [^{19}F]-KF.

Following up on our communication, we sought alternate means besides avidin- affinity chromatography for removing free fluoride from small-molecule compositions containing an [^{18}F]-ArBF$_3$. Having discovered that the NH$_4$OH:EtOH TLC system separated the ArBF$_3$ from free fluoride, we recognized that the *p*-biotinamidophenyltrifluoroborate exchanged its fluoride very rapidly, consistent with the data presented herein, and in stark contrast to the conclusions we had initially reported.

Although our initial communication indicated that we had prepared a substance derived from a boronic acid that labeled in the presence of aqueous [^{18}F]-fluoride and manifested suitable stability, in light of the data we report herein, we speculate that the high molar ratios of *p*-biotinamidophenyltrifluoroborate: avidin in our earlier report may have contained trace impurities, on the order of 1%, which may have adventitiously bound to the avidin magnetic particles leading us to overestimate the aqueous stability of the target *p*-biotinamidophenyltrifluoroborate. Nevertheless, the conclusions of that preliminary work proved conceptually and qualitatively correct: to apply this approach for *in vivo* imaging we needed to identify a class of ArBF$_3$s that would be considerably more stable over the time that a physiological process is imaged. Thus, the results and analysis herein, which reflect a reinvestigation of earlier claims, disclose the scientific process and theory that now allow the development of solvolytically robust ArBF$_3$ compositions. Indeed, based on the findings now assembled here, we have recently reported the synthesis of a fluorescently (BODIPY) linked 1,3,5-trifluoro-2-carboxamidophenyl-6-[^{18}F]-trifluoroborate, which exhibits extraordinary *in vitro* stability (k_{obs} for solvolysis $\sim 10^{-4}$ min.$^{-1}$)[54] and will report on the *in vivo* stability of a biotinylated derivative thereof in the near future.

For those who are skeptical of preparing viable trifluoroborate-based PET-imaging agents in the presence of added carrier, we reiterate our original claims that ArBF$_3$s can be generated under no-carrier-added conditions but not in carrier-free form. To dispel this skepticism, we review the underlying thermodynamics of ArBF$_3$ synthesis given in equation 1.

$$K_{eq}(\text{formation pH 4}) = \frac{[ArBF_3]}{[ArB(OH)_2][F^-]^3} \qquad (1)$$

On the basis of eq 1, radiosynthetic yields exhibit third-order dependence on fluoride concentration. Yield notwithstanding, le Chatelier's principle holds that some ArBF$_3$ must necessarily form irrespective of the fluoride concentration used. At 100 mM fluoride, ArBF$_3$ formation is relatively fast, and in our hands, chemical yields with respect strongly EWG-containing arylboronic acids have varied from 10% to 50% over the period of 1 h and higher yields are obtained over longer times. Nevertheless, because relatively high concentrations are needed, low volumes may be necessary to ensure high yields when using no-carrier-added fluoride.

In critically evaluating the potential of this approach for labeling with no-carrier-added fluoride, in particular with regards to isotopic purity and yields, the reader must note that a no-carrier-added [^{18}F]-fluoride is *never* carrier-free because of the adventitious presence of contaminating environmental [^{19}F]-fluoride, which, in practice, dramatically reduces the specific activity to $\sim$100 Ci/μmol, if not considerably lower.[55] At $\sim$100 Ci/μmol, only 5 of 86 fluoride ions are radioactive such that the resulting ArBF$_3$ will represent a statistical mixture of inseparable istopologs where 99% of all species are unlabeled and monolabeled, with less than 1% containing more than 1 radioactive ^{18}F-atom.[56] Such a distribution is not dissimilar from other labeling strategies that rely on C−F bond formation. In addition, 1 Ci will contain >10 nmol total fluoride, which means that the reaction can be run in a tenable volume of 100 nL, using a microfluidic reactor to ensure a solution of 100 mM fluoride.[57] Furthermore, the 3-to-1 stoichiometry of conversion stipulates that the specific activity of the resulting ArBF$_3$ will be thrice that of the fluoride used, irrespective of either the fluoride concentration or the yield of the resultant ArBF$_3$. Besides the question of yield is one of purity; this work also demonstrates that no stable mono- or difluoridated species are produced in this labeling scheme, which provides for a chemically pure aryltrifluoroborate salt.

Finally, it is essential to note that the most important concern for imaging an extracellular receptor with a radiolabeled ligand is the final specific activity of the labeled ligand, which must be >1 Ci/μmol, and not the specific activity of the fluoride used initially. Thus, a synthesis in which 1 Ci of fluoride is supplemented with $\leq$1μmol of [^{19}F]-fluoride still satisfies the specific activity requirements for imaging yet allows the radiochemist to expect reasonable yields when working in volumes as high as 10 μL.

Experimental Section

ArBF$_3$ Synthesis. For nonradioactive samples, ArBF$_3$s were converted from their corresponding commercially available boronic acids or boron pinacol esters in the presence of KHF$_2$ and were isolated through acetonitrile or methanol washes according to procedures described by Vedejs[58] and Molander.[59] Certain ArBF$_3$s could not be completely separated from free fluoride without concomitantly large losses of ArBF$_3$. As these are considered commonly in use, the spectra are reported in the Supporting Information.

The *p*-(CH$_3$)N$^+$PheBF$_3^-$ (*p*-trimethylammoniophenyltrifluoroborate) was unknown in the literature and synthesized as with the other ArBF$_3$s from its precursor pinacolate: ^{1}H NMR (400 MHz DMSO-d_6) δ 7.6 (d, J = 8 Hz, 2H), 7.5 (d, J = 8 Hz, 2H), 3.3 ppm (s, 9H); ^{19}F NMR (400 MHz DMSO-d_6) δ −62.5 ppm (quadrapolar coupling to boron not observed). The precursor was the *p*-trimethylammoniophenylboronylpinacolate, which was prepared by reacting commercially available *p*-*N*,*N*-dimethylaminophenylboronylpinacolate (700 mg) in neat CH$_3$I (1 mL) for 12 h. The

(54) Ting, R. et al. *J. Fluorine Chem.* **2008,** *129*, 349−358.

(55) Reference 52.

(56) The statistical breakdown is where approximately 83.55% will be unlabeled, 15.47% will be mono-labeled, 0.951% will be bis-labeled, and 0.0195% will be tris-labeled.

(57) If one considers the hypothetical case of using 1 Ci of carrier free [^{18}F]-fluoride (581 pmol, specific activity 1720 Ci/μmol), one would have to employ 5 pL reaction volumes to achieve the same yields—a veritable challenge that may be met with microfluidic reactors. Whatever amount of ArBF$_3$ that forms with carrier-free [^{18}F]- fluoride will necessarily be 100% ^{18}F-labeled. In this hypothetical case, the resulting ArBF$_3$ will contain three atoms of [^{18}F]-fluoride and not only one.

(58) Vedejs, E.; Chapman, R. W.; Fields, S. C.; Lin, S.; Schrimpf, M. R. *J. Org. Chem.* **1995**, *60*, 3020–3027.

(59) Molander, G. A.; Bernardi, C. R. *J. Org. Chem.* **2002**, *67*, 8424–8429.

precipitate was collected, washed with CH_2Cl_2, pumped dry of residual CH_3I, washed with Et_2O, and then placed on high vacuum overnight; ^{1}H NMR (400 MHz CD_2Cl_2) δ 8.0 (d, J = 8 Hz, 2H), 8.0 (d, J = 8 Hz, 2H), 4.0 (s, 9H), 1.3 ppm (s, 12H); HRMS (M + K)$^+$ calcd $C_9H_{13}BNF_3K^+$ 242.0730 *m*/*z*, found 242.0724.

^{19}F NMR Spectroscopic Kinetic Analyses. All ^{19}F NMR spectra are referenced to TFA. A small quantity of the isolated $ArBF_3$ salt (~0.3−1 mg or 1−5 μmol) was added to a Norell 507-HP NMR tube. At t = 0 min, the start of the solvolysis reaction, the $ArBF_3$ was dissolved in 500 μL of a 192 mM pH 6.9−7.0 phosphate buffer (resulting in a 2−10 mM solution) and decomposition was monitored by ^{19}F NMR spectroscopy. ^{19}F NMR spectra were acquired at different times. ^{19}F NMR spectral integrations were calculated on obtained spectra, using MestReC NMR spectral data processing software. Integrals corresponding to the $ArBF_3$ peak were divided by the sum of the $ArBF_3$ and free fluoride integrations to calculate the fraction of ^{19}F existing as the $ArBF_3$. The ratio of ^{19}F signal existing as the $ArBF_3$ to the total ^{19}F signal was plotted against time in eq 1 to calculate, k_{obs}, the observed first-order rate constant for loss of [^{19}F]-fluoride from $ArBF_3$. A half-life for this process was calculated by setting $t_{1/2}$ = (ln 2/k_{obs}). The kinetic constants reported in this text are the result of nonlinear regression analyses of the cumulative plot of all data sets for identical experiments using the Sigma Plot 2001 v7.101.

[^{18}F]-Fluoride Preparation. The desired activity of [^{18}F]-fluoride was prepared via bombardment of 1 mL of $H_2{}^{18}O$ water with 13 MeV protons in a niobium target. To recover unconverted $H_2{}^{18}O$, the resulting [^{18}F]-fluoride/$H_2{}^{18}O$ solution was passed through a short anion-exchange resin (~10 mg, CO_3^{2-} form). Resin-bound fluoride was eluted with 200 to 300 μL of 1 mg/mL aqueous $NaClO_4$ and recovered in a glass vial. Depending on the desired activity, this sample could be diluted with deionized water or used as is, or the sample could be concentrated through heating under vacuum. Usually 1−6 mCi were used to which carrier [^{19}F]-fluoride was added and then diluted accordingly. **Hazard Note:** Care must be taken in acidifying and concentrating [^{18}F]-fluoride containing water. If the pH is adjusted lower than 3, a radioactive and volatile HF vapor is produced. Use of a fumehood with filtered air flow is recommended.

Although $NaClO_4$ is a known oxidant, it was used instead of carbonate as an elutant because (i) it is a more powerful elutant than carbonate and (ii) minimized the presence of eluted carbonate that often rendered the resulting [^{18}F]-fluoride solution quite basic, i.e., pH >9. Since 20 μCi was used (*vide infra*), this represented a >50-fold dilution of the perchlorate. As such, were all of the perchlorate to pass through the column, the maximum amount of perchlorate available in the fluoridation reaction would be 12 mM—far less than the boronic acid used. At these concentrations the extent to which perchlorate could interact (and thus diminish) with the arylboronate species was considered negligible.

[^{18}F]-$ArBF_3$s were synthesized by incubating 5 μL of a 200 mM boronic acid/ester solution in DMF with 5 μL of 400 mM KHF_2 solution pH 3−4, containing a minimum of ~20 μCi of [^{18}F]-fluoride (specific activity at the start of reaction). The mixing of these solutions resulted in a 10 μL cocktail containing 100 mM boron and 200 mM KHF_2 containing [^{18}F]-fluoride. This solution will be referred to herein as "Reaction A" and the time at which these two solutions were mixed will be referred to as the start of the fluoridation reaction (t = 0 min). All described experiments requiring [^{18}F]-fluoride did not exceed t = 6 h or ~ 3 half-lives of decay. Typically the 400 mM KHF_2 solution is made up in a cocktail format, where 40 μL of 4 M KHF_2 and 20 μL of 2 M HCl in order to neutralize any CO_3^{2-} that eluted as a counterion from the anion exchange resin are added to 340 μL of ~3 mCi [^{18}F]-fluoride in H_2O. With the large excess of [^{19}F]-fluoride carrier added in the conditions described, the [^{18}F]-$ArBF_3$ species is constituted (>99.99%) by a uniquely labeled isotopolog $ArB[^{18}F][^{19}F]_2$ containing a single atom of [^{18}F]-fluorine.

To assay the solvolysis rate of [^{18}F]-fluoride from [^{18}F]-$ArBF_3$, the [^{18}F]-$ArBF_3$s featured in Table 1 (Supporting Information) were prepared as described for "Reaction A". One hour (t = 60 min) following fluoridation, a volume of 1.5 μL was taken from "Reaction A" and diluted 200 times into 300 μL of a 192 mM PO_4 pH 6.9−7.0, 100 mM [^{19}F]-KF solution. A series of dilution experiments corresponding to different solvolysis times were made from the same $ArBF_3$ cocktail at times that were staggered such that all reactions were terminated at the same end point and resolved by TLC. At this end point, 0.5 μL of each reaction was spot on a TLC plate, which was run ~5 cm in a 5% NH_4OH/EtOH developing solution.

Kinetic Analysis with ^{18}F/^{19}F TLC Autoradiography. To ensure that all samples were resolved at the same time by TLC, kinetics of solvolysis in excess [^{19}F]-fluoride were initiated for different lengths of time, e.g., 199, 134, 80, 62, 46, and 31 min, prior to TLC resolution (see Figure 3). Of note, while complete conversion of the arylboronic acid/ester to the $ArBF_3$ is not required for this assay, it is essential that the ratio of $ArBF_3$:fluoride in "Reaction A" be constant for each time point represented in the ^{18}F/^{19}F-exchange reaction and not be increasing over time. This condition was thus verified even though previous reports suggested that boronic acids or boron pinacol esters are quantitatively converted to $ArBF_3$s in aqueous solutions of 200 mM KFH_2 and this conversion occurs between 1 and 60 min. To verify that fluoridation was rapid, kinetic profiles of $ArBF_3$ formation were first monitored by TLC-autoradiography in the following manner: three different reactions were initiated and allowed to proceed for various times, t = 240, 60, and 30 min. All three reactions were then stopped within a minute or two of each other by spotting 0.3 μL of each reaction on a TLC plate, which was run 5−6 cm with 5% NH_4OH/EtOH as the running solvent. All arylboronic acids/esters gave rise to $ArBF_3$s that exhibited R_f values of 0.75−0.95 in this developing solution, with the exception of the *p*-$(CH_3)_3N$-$PheBF_3$, which did not migrate appreciably from the baseline (data not shown). Autoradiographic assays on very early time points, e.g., 1−5 min, showed variable but usually minor amounts of $ArBF_3$; however, by 30 min $ArBF_3$ synthesis was generally complete and no more $ArBF_3$ had formed at longer time points. Furthermore, in no case was any intermediate observed by autoradiographic analysis. On the basis of these tests, we concluded that $ArBF_3$ formation for all members of the assayed library was complete within 30 min (data not shown).[60] Furthermore, spotting and drying on the TLC plate for 30 min had little effect compared to freshly spotted reactions. Thus, we verified that the concentration of components upon drying on the TLC plate did not result in substantially more conversion of the $ArBF_3$.

Autoradiography of [^{18}F]-$ArBF_3$s and [^{18}F]-fluoride was accomplished by exposing TLC plates on Molecular Dynamics phosphor screens overnight and scanning the screens on a Molecular Dynamics Typhoon 9200 phosphoimager. Polygons were drawn around distinct spots with ImageQuant v. 5.2. Time values noted in the figures concerning the isotopic ^{18}F/^{19}F-fluoride exchange experiments were the times that [^{18}F]-$ArBF_3$s remained diluted in the phosphate solution.

Data were entered into Excel Spreadsheets and graphed in either Excel or SigmaPlot. Using the LINEST function in Excel, Hammett plots were generated from a simple one-variable linear regression and Yukawa−Tsuno plots were generated with a double variable linear regression according to $\log(k_{obs}) = \rho\sigma^+ - R'\Delta\sigma$, where $R' = \rho R$ and $\Delta\sigma$ is the difference between reported values of σ^+ and σ.

(60) Indeed, had this not been the case and the $ArBF_3$ concentration were increased between the start of the ^{18}F/^{19}F-exchange reaction representing a long time point (e.g., 199 min) and the end of the exchange reaction representing a short time point (e.g., 31 min), such would actually lead to an overestimation of the rate constant for solvolysis.

Acknowledgment. R.T. was the recipient of a Gladys Estella Laird and a Michael Smith Foundation for Health Research Ph.D. traineeship. D.M.P. received a Michael Smith Career Scholar Award. D.M.P. thanks Prof. Charles L. Perrin and Dr. Marilyn H. Perrin for insightful discussions. This work was supported by the Canadian Institutes for Health Research.

Supporting Information Available: Detailed methods, spectra, autoradiography, and Table 1 containing data for Hammett plots. This material is available free of charge via the Internet at http://pubs.acs.org.

JO800681D